Uncertainties propagation in metamodel-based probabilistic optimization of CNT/polymer composite structure using stochastic multi-scale modeling

Hamid Ghasemi[1], Roham Rafiee[2], Xiaoying Zhuang[3], Jacob Muthu[4],Timon Rabczuk*[1, 5]**

[1] Institute of Structural Mechanics, Bauhaus University Weimar, Marienstraße 15, 99423 Weimar,Germany
[2] Composites Res. Lab., Faculty of New Sci. & Tech., University of Tehran, Tehran, 1439955941, Iran
[3] Dep. of Geotech. Eng., College of Civil Eng., Tongji Uni., 1239 Siping Road, Shanghai 200092, China
[4] School of Mechanical, Industrial and Aeronautical Eng., Uni. of the Witwatersrand, WITS 2050, S. Africa
[5] Professor at (1) and School of Civil, Environmental and Architectural Eng., Korea University, Seoul, S. Korea

Abstract

This research focuses on the uncertainties propagation and their effects on reliability of polymeric nanocomposite (PNC) continuum structures, in the framework of the combined geometry and material optimization. Presented model considers material, structural and modeling uncertainties. The material model covers uncertainties at different length scales (from nano-, micro-, meso- to macro-scale) via a stochastic approach. It considers the length, waviness, agglomeration, orientation and dispersion (all as random variables) of Carbon Nano Tubes (CNTs) within the polymer matrix. To increase the computational efficiency, the expensive-to-evaluate stochastic multi-scale material model has been surrogated by a kriging metamodel. This metamodel-based probabilistic optimization has been adopted in order to find the optimum value of the CNT content as well as the optimum geometry of the component as the objective function while the implicit finite element based design constraint is approximated by the first order reliability method. Uncertain input parameters in our model are the CNT waviness, agglomeration, applied load and FE discretization. Illustrative examples are provided to demonstrate the effectiveness and applicability of the present approach.

Keywords: Reliability Based Design Optimization (RBDO), Reliability Analysis, Carbon Nano Tube (CNT), Multi-Scale Modeling, CNT/Polymer Composite

1. Introduction

CNT/Polymer composites have received attention thanks to their enhanced mechanical, electrical and thermal properties [1]. Different approaches have been used in order to characterize PNCs: atomistic modeling, continuum modeling (which can be also subdivided into analytical and numerical approaches) and multi-scale methods [2]. Molecular dynamics

---

*Corresponding Author: Tell: (+49)3643-584511, E-Mail: timon.rabczuk@uni-weimar.de
**Second corresponding author: E-mail: Roham.Rafiee@ut.ac.ir

(MD) simulations restrict the model to one CNT in a polymer matrix with very short length. Pure continuum modeling approaches which usually deal with evaluating the composite response in the scale of a Representative Volume Element (RVE), don't account for phenomena taking place on finer scales. Therefore, multi-scale methods were employed coupling MD methods and continuum methods. An overview of Multi-scale methods for PNCs has been presented in [3].

The characteristics of a Carbon Nano Tube Reinforced Polymer (CNTRP) material are influenced by many uncertainties. These uncertainties include material properties, the geometry, loading and boundary conditions and the model uncertainties. Hence, probabilistic approaches are needed to determine the reliability of the behavior of nanocomposite structures.

In this research work, uncertainties are classified in three major groups: material uncertainties, structural uncertainties and modeling uncertainties (Fig. 1). Material uncertainties include the molecular interactions and the CNT diameter at nano-scale, the CNT length and CNT-resin interaction at micro-scale, the CNT content, agglomeration, curvature, orientation at meso-sclae and the CNT dispersion at macro-scale. Each component e.g. the resin can also experience uncertainties in its material properties (such as Young's modulus and Poisson's ratio). Structural uncertainties lie for instance in the geometry, boundary and loading conditions while typical model uncertainties concern the mathematical model, the discretization and approximation errors. These uncertainties will propagate over different length scales affecting the overall reliability of the structural component.

Uncertainty propagation in nanocomposite structures remains an unsolved issue. Rouhi and Rohani [4] measured the failure probability of a nanocomposite cylinder under buckling, accounting for uncertain design conditions. However, they used micromechanical equations at the nano-scale by simply replacing the lattice structure of a CNT with a solid fiber (which can lead to inappropriate results [2]). Moreover, they disregard several important CNT parameters such as the CNT length, diameter, agglomeration and dispersion without any sensitivity evaluation. Furthermore, modeling errors including discretization- and approximation errors have not been addressed in detail. Motivated by [4], this research work firstly considers the most feasible uncertain design parameters and variables in the model in order to get a more realistic insight towards uncertainties and their effects on the final nanocomposite product design. Secondly, it extends the design optimization of nanocomposite components from a pure geometry-oriented approach to a material-orientated

approach and a "hybrid approach" accounting for the simultaneous optimization of the geometry and material.

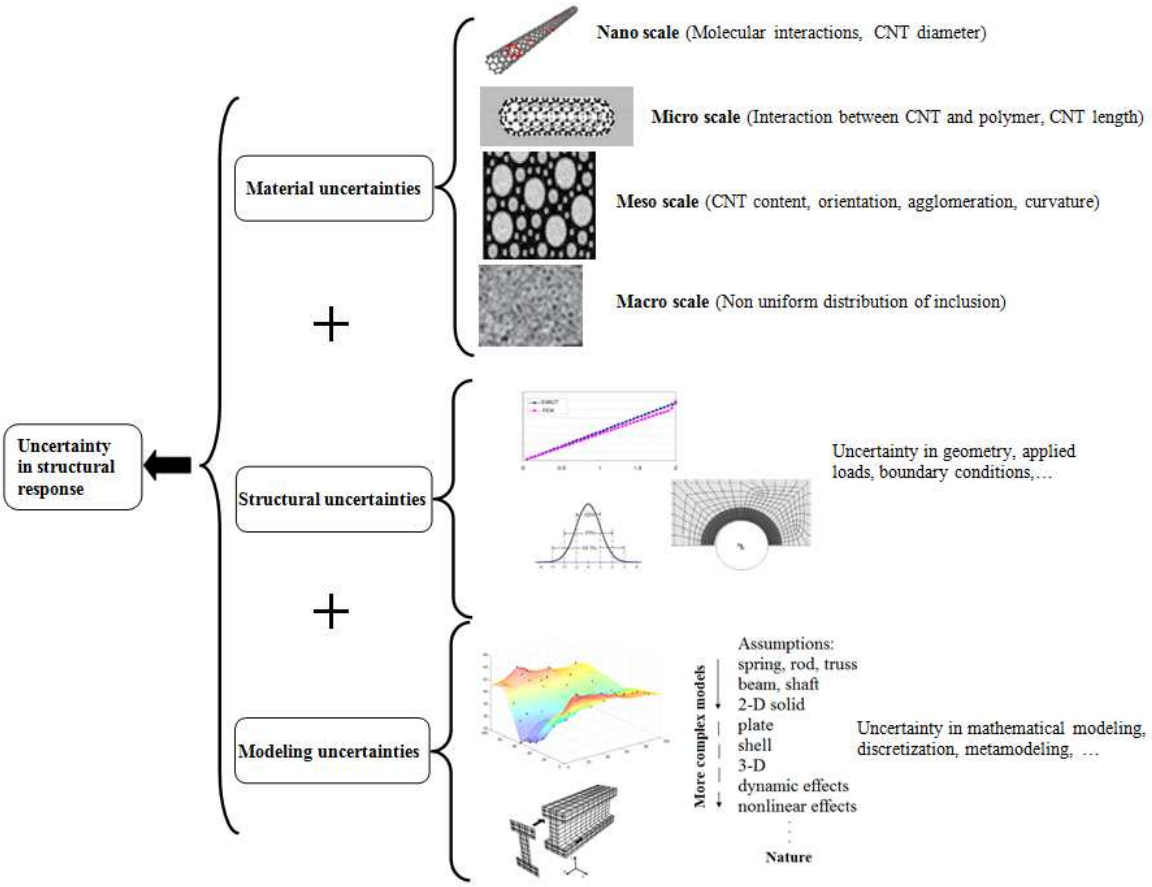

Fig.1. Uncertainities sources and their propogation over differents length scales and sources

For a specific load, the optimal structural results obviously will be obtained for idealistic straight, aligned and not aggregated CNTs. Perfect manipulation of these parameters with current technologies seems to be impractical. On the other hand, the behavior of CNTRP can be changed more efficiently by varying the content of the CNT rather than changing other parameters. To our best knowledge, this is the first approach optimizing the CNT content in generic nanocomposite solids considering nearly all CNT parameters. It will answer the question how much CNTs should be added to a resin for an optimal and reliable response of the structural component.

The manuscript is organized as follow: Section 2 presents an overview of the stochastic multi-scale material model. The reliability concept and the implemented metamodeling technique are described in Sections 3 and 4, respectively. Section 5 discusses the Reliability Based Design Optimization (RBDO) and approximation based RBDO, while Section 6 contains some case studies. The concluding remarks are presented in Section 7.

2. Stochastic multi-scale CNT/polymer material model

The stochastic multi-scale model has been adopted from [5,6,7]. Fig. 2 illustrates the bottom-up approach including bridging the nano-scale up to the macro-scale (N3M).

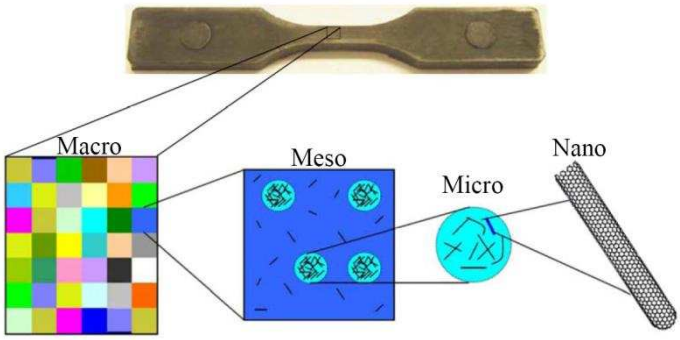

Fig.2. Involved scales in simulation of CNTRP [5]

The CNT is modeled by a quasi-continuum method using beam elements at the nano-scale. Therefore, the strain energy of the beam elements is equated to the interatomic potential energy of Carbon-Carbon (C-C) bonds accounting for the 3-D frame structure of the molecular lattice. Using beam elements instead of spring or truss elements reduces the number of elements in the FE model and consequently reduces the computational cost (to find reasons reader can refer to [5]). Neglecting electrostatic interactions between the CNTs and the surrounding matrix, the interphase region is modeled by non-bonded van der Waals (vdW) interactions. The polymer matrix of the PNC is based on a continuum model at the micro-scale as shown in Fig. 3. The interphase behavior is modeled by the adaptive vdW Interaction (AVI) based on 3D truss elements [6]. The material behavior of the micro-model is up-scaled by developing the concept of equivalent fibers accounting for different CNT-length and the complex interphase behavior[6].

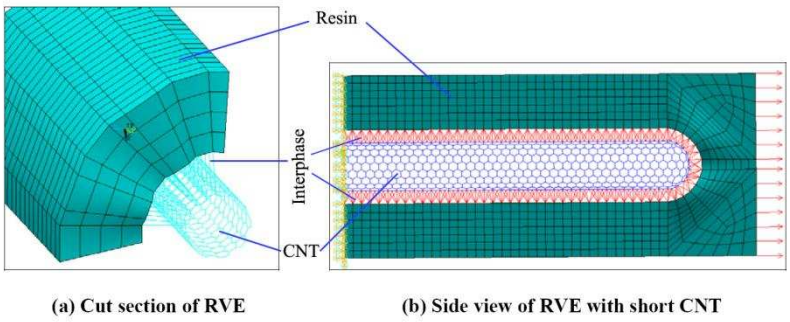

Fig.3. Cuncurrent multi-scale FE model of RVEs as micro-scale [5]

Randomly distributed and orientated embedded equivalent fibers at meso-scale can experience straight and wavy forms. They can be also concentrated in local aggregates or dispersed in some other areas. A schematic view of RVE at meso-scale is shown in Fig. 4. Using equivalent fiber technique, micromechanics theories can be used at proper scale of meso instead of nano. So, implementing improved micromechanics model by Shi [8], based on Mori-Tanaka model [9], the Young's modulus and Poisson ratio of the block of Fig. 4 can be obtained. The effect of the CNT waviness (the state of non-straight shape of CNT) is also captured by considering upper and lower bounds of longitudinal and transverse stiffness. More details about waviness modeling are presented in Section 6.1.

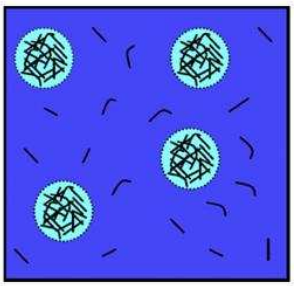

Fig.4. RVE of composite at meso-sclae [5]

A Voigt model has been used to determine the overall properties of the material region at the macro-scale. Monte Carlo Simulations (500 realization on an 80×80 material region mesh), for the N3M multi-scale model account for the stochastic uncertainties in CNTRP. The N3M algorithm is summarized in Fig. 5.

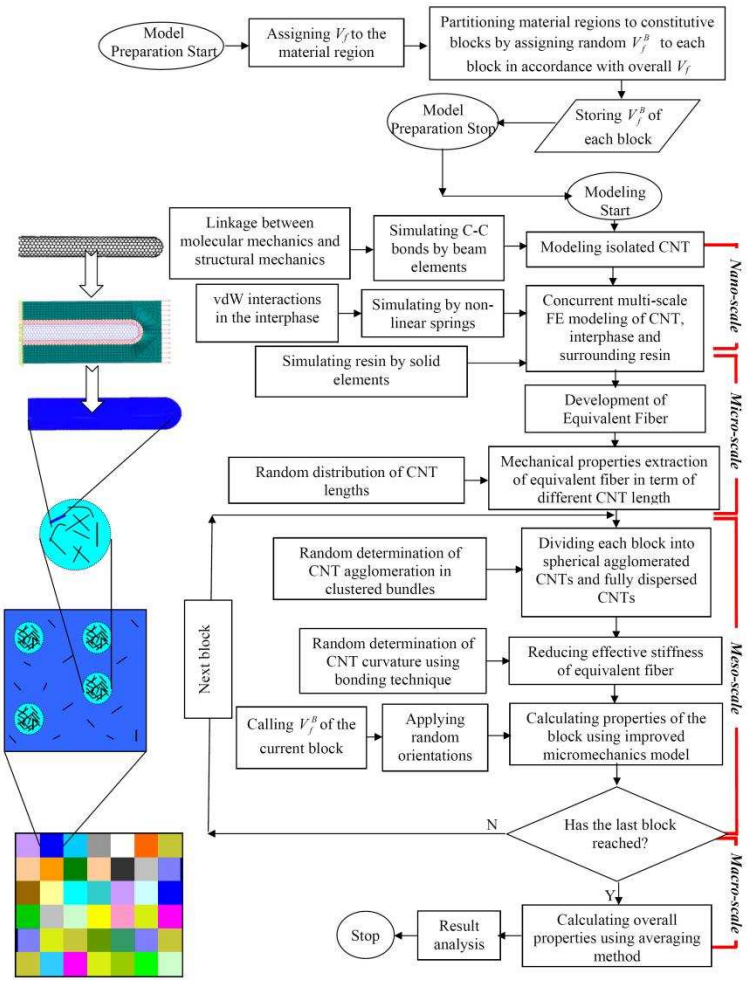

Fig.5. Flowchart of developed full stochastic N3M multi-scale material model [5]

3. Structural reliability

Fig. 6 shows the structural safety concept. Let L and R being the system response and resistance of a structural component, respectively. Thus, the system is safe for $L < R$. The nominal safety factor is defined as $S.F. = \frac{R_{nom}}{L_{nom}}$ where R_{nom} and L_{nom} are conservative values (e.g. 2-3 standard deviation below and above the mean, respectively). The nominal safety factor may not exactly present the safety margin in a design and it can lead to either catastrophic failure or unnecessary conservatism. Therefore, the concept of failure probability was introduced.

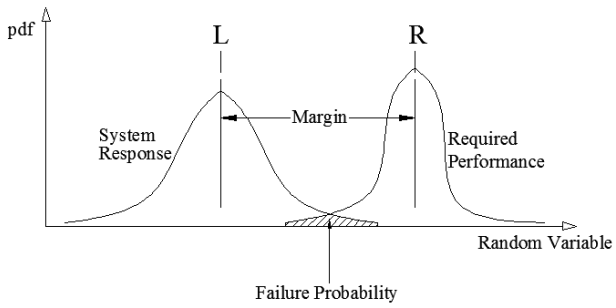

Fig.6. Concept of structural safety and failure probability

According to probability theory, a random event $\boldsymbol{A}$ can be defined by the occurrence of a real-valued random value $\boldsymbol{X}$, which is smaller than a prescribed deterministic value x:

$$\boldsymbol{A} = \{\boldsymbol{X} | \, \boldsymbol{X} < x\} \tag{1}$$

The Cumulative Distribution Function (CDF) indicated by $F_{\boldsymbol{X}}(x)$, relates the probability of $[\boldsymbol{A}]$ to x:

$$F_{\boldsymbol{X}}(x) = Prob[\boldsymbol{A}] = Prob[\boldsymbol{X} < x] \tag{2}$$

Since $-\infty < x < +\infty$, then $\lim_{x\to-\infty} F_{\boldsymbol{X}}(x) = 0$ and $\lim_{x\to+\infty} F_{\boldsymbol{X}}(x) = 1$. The so-called Probability Density Function (PDF) is defined by taking derivatives of $F_{\boldsymbol{X}}(x)$ with respect to x, (i.e. $f_{\boldsymbol{X}}(x) = \frac{d}{dx} F_{\boldsymbol{X}}(x)$). Finally, the failure probability is presented by

$$P_f = Prob[g(x) \leq 0] \tag{3}$$

and in its general form:

$$P_f = Prob[g(x_1, x_2, \dots, x_n) \leq 0] = \int_{g(x)\leq 0} \dots \int f_{\boldsymbol{X}}(x) dx \tag{4}$$

where $g(.)$ is the limit state function (LSF) and $g(.) \leq 0$ denotes a subset of the outcome space, where failure occurs. The difficulty in computing Eq. (4) has led to the development of various approximation methods. One of the most popular approaches is the First Order Reliability Method (FORM). An excellent overview of available methods for structural reliability analysis is given in [10] and references therein.

FORM approximates the LSF by a first order Taylor expansion at the Most Probable Point (MPP), the point in the normal space with the highest density on the LSF (see Fig. 7):

$$\tilde{g}(x) = g(\mu_{\boldsymbol{X}}) + \nabla g(\mu_{\boldsymbol{X}})^{\mathrm{T}} (x - \mu_{\boldsymbol{X}}) \tag{5}$$

It can be also shown that:

$$\mu_{\tilde{g}} = g(\mu_{\boldsymbol{X}}) \quad \text{and} \quad \sigma_{\tilde{g}} = \left[\sum_{i=1}^{n} \left(\frac{\partial g}{\partial x_i} \right)^2 \sigma_{x_i}^2 \right]^{1/2} \tag{6}$$

where $\mu_{\boldsymbol{X}}$ and σ_{x_i} are the mean value and standard deviation of random variables, respectively. Hasofer and Lind [11] presented the current concept of Reliability Index (β), based on the shortest distance from the origin of reduced variables to the limit state surface. Mathematically it is described by a minimization problem with an equality constraint:

$$\begin{cases} \beta = \min(\boldsymbol{U}.\boldsymbol{U}^T)^{\frac{1}{2}} \\ s.t: \\ g(\boldsymbol{U}) = 0 \end{cases} \tag{7}$$

which leads to the Lagrange-function:

$$L = \frac{1}{2}\boldsymbol{U}^T\boldsymbol{U} + \lambda g(\boldsymbol{U}) \rightarrow \ minimize \tag{8}$$

Solving Eq. (8) results in finding $\boldsymbol{U}_{MPP}$ which corresponds to the highest value of the PDF as shown in Fig. 7. It should be emphasized that FORM requires standard normal non-correlated variables; so the vector of random variables $\boldsymbol{X}$ must be transformed into the standard non-correlated variables vector $\boldsymbol{U}$:

$$\boldsymbol{U} = \Phi^{-1}\big(F_{\boldsymbol{X}}(x)\big) \tag{9}$$

The reliability R and the corresponding failure probability P_f can be expressed as:

$$R = \Phi(\beta) \tag{10.a}$$

$$P_f = 1 - R = 1 - \Phi(\beta) = \Phi(-\beta) \tag{10.b}$$

where Φ and Φ^{-1} are the standard cumulative distribution function and its inverse for the vector of normal variables $\boldsymbol{X}$, respectively.

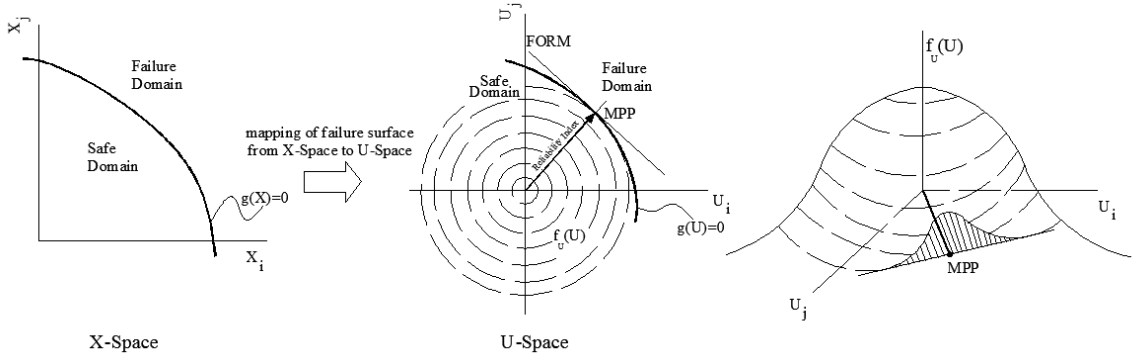

Fig.7. Graphical representation of the FORM approximation

4. Metamodeling

4.1. Concept and application

In simulation-based optimization, implicit forms of objective functions and constraints dealing with either gradient based or gradient free optimization techniques are computationally expensive, particularly with increasing number of variables and function evaluations. In order to improve the computational efficiency in such design problems, the concept of "metamodel" approximating the physical model has been introduced. The metamodel is constructed based on a sufficient number of sampling points, typically determined through experiments. Selecting a Design Of Experiment (DOE) method for data generation, choosing a model to represent the data, fitting the model and finally model validation are the four basic steps in metamodeling [12]. In this research work, the kriging method [13] has been utilized to approximate our multi-scale material model.

4.2. Kriging method

In the kriging method, the unknown value of a response for an input sample point should be the weighted average of the known values of the responses at its neighbors. The basic form of the kriging estimator is:

$$Z^*(\boldsymbol{u}) - m(\boldsymbol{u}) = \sum_{\alpha=1}^{n(\boldsymbol{u})} \lambda_\alpha [Z(\boldsymbol{u}_\alpha) - m(\boldsymbol{u}_\alpha)] \tag{11}$$

where $Z(\boldsymbol{u})$ is the random field with a trend component $m(\boldsymbol{u})$ and a residual component $R(\boldsymbol{u}) = Z(\boldsymbol{u}) - m(\boldsymbol{u})$; $\boldsymbol{u}$ being the location vector for an estimation point; $n(\boldsymbol{u})$, $m(\boldsymbol{u})$ and $\lambda_\alpha(\boldsymbol{u})$ are the number of data points in the local neighborhood of the estimated point, the expected (mean) value of $Z(\boldsymbol{u})$ and the assigned kriging weights, respectively. The superimposed * also indicates estimated value. The goal is to determine the weights, λ_α, that minimize the variance of the estimator:

$$\sigma_E^2(\boldsymbol{u}) = Var\{Z^*(\boldsymbol{u}) - Z(\boldsymbol{u})\} = 0 \tag{12}$$

under the unbiased constraint $\mathbb{E}\big(Z^*(\boldsymbol{u}) - Z(\boldsymbol{u})\big) = 0$, where $\mathbb{E}(.)$ is the expected value or ensemble average. A computer implementation of the kriging method [14] has been used to find the unknown weights, λ_α. Fig. 8 (a) compares actual and estimated values of CNTRP stiffness obtained by N3M and metamodel, respectively. Fig. 8 (b) shows mean squared error for each predicted point. It can be observed that N3M model can be substituted by kriging metamodel with high level of accuracy and very cheap computational cost.

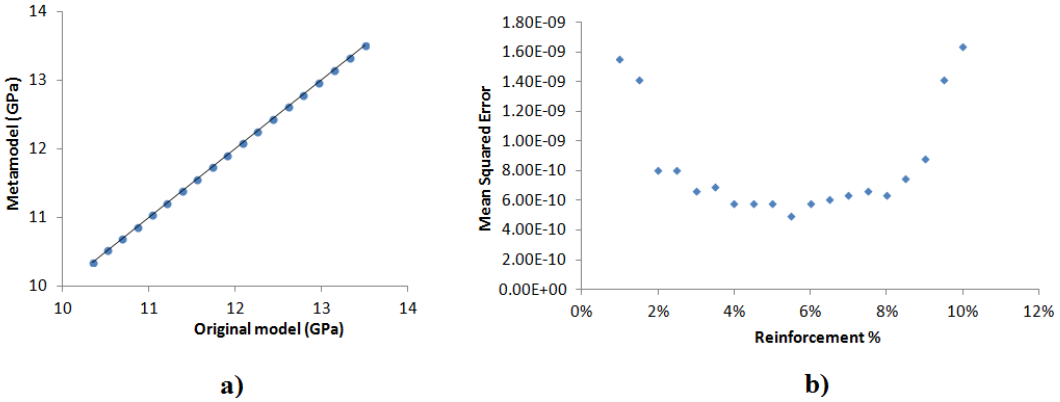

Fig.8. Verification of the metamodel (a) mean squared error of each predicted point (b)

5. RBDO and metamodel-based RBDO

Uncertainties influencing the material and structural response of nanocomposites call for optimization models which can capture the effects of random variables and yield to reliable designs with higher level of confidence. In contrary to Determinstic Design Optimization (DDO), in RBDO, design parameters are random variables and the optimization objective function is subjected to probabilistic constraints.

Fig. 9 schematically compares RBDO and DDO. In DDO almost 75% of the designs around the deterministic optimum fail while RBDO finds the optimal design allowing a specific risk and target reliability level by accounting for the stochastic nature of the random parameters.

In its basic form the problem of RBDO can be presented as below:

$$\min_{\boldsymbol{\theta}} C(\boldsymbol{\theta})\ s.t.\ \begin{vmatrix} f_1(\boldsymbol{\theta}), \dots, f_{q-1}(\boldsymbol{\theta}) \le 0 \\ f_q(\boldsymbol{X}, \boldsymbol{\theta}) = \beta_t - \beta(\boldsymbol{X}, \boldsymbol{\theta}) \le 0 \end{vmatrix} \tag{13}$$

where $\boldsymbol{\theta}$ is the vector of the design variables with the mean value of the random variable $\boldsymbol{X}$, $C(\boldsymbol{\theta})$ is the cost or objective function, $f_1(\boldsymbol{\theta}), \dots, f_{q-1}(\boldsymbol{\theta})$ is a vector of $(q-1)$ deterministic constraints over the design variables $\boldsymbol{\theta}$, $f_q(\boldsymbol{X}, \boldsymbol{\theta})$ is the reliability constraint enforcing the respect of LSF and considering the uncertainty to which some of the model parameters $\boldsymbol{X}$ are subjected to. β_t is the target safety index.

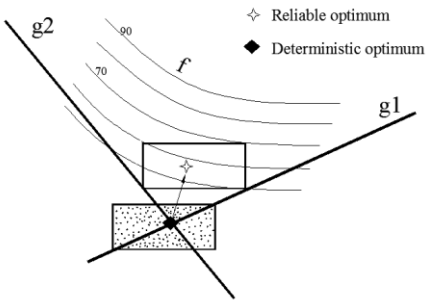

Fig.9. Schematic comparisons between RBDO and DDO, f stands for objective function

In this research a kriging based metamodel has been utilized in each RBDO iteration. In other words: instead of carrying out the RBDO process with the original multi-scale material model, the approximation based RBDO is conducted with the metamodel. If the function expressing the true nature of the computer analysis result is $y = f(x)$, the metamodel of the computer analysis is $\hat{y} = \hat{f}(x)$, and hence $y = \hat{y} + \varepsilon$, where ε is the error of the approximation. So, the metamodel-based RBDO becomes:

$$\min_{\boldsymbol{\theta}} \hat{C}(\boldsymbol{\theta})\ s.t. \begin{vmatrix} \hat{f}_1(\boldsymbol{\theta}), \ldots, \hat{f}_{q-1}(\boldsymbol{\theta}) \le 0 \\ \hat{f}_q(\boldsymbol{X}, \boldsymbol{\theta}) = \beta_t - \beta(\boldsymbol{X}, \boldsymbol{\theta}) \le 0 \end{vmatrix} \tag{14}$$

Eq. (14) has been solved by the open source software FERUM 4.1 [15] and linked to our FE code which evaluates the LSF numerically. The FERUM v4.1 toolbox involves a nested, double-loop solution procedure where the outer optimization loop includes inner loops of the reliability analysis. In each reliability analysis, the reliability index approach is used as a separate optimization procedure in the standard normal space to search for the most probable point for each active probabilistic constraint. Fig. 10 illustrates the nested algorithm of the RBDO procedure.

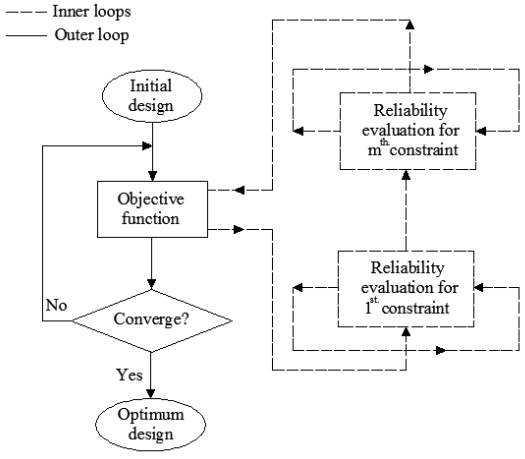

Fig.10. Double loop RBDO flowchart

6. Case studies

In our case studies, firstly the RBDO is employed to find the optimal content of CNT as well as the optimal geometry of a nancomposite component; and secondly, the sensitivity of the structural failure probability with respect to uncertain design variables is quantified. The two subsequent examples will show how the uncertainties influence the optimization of the structural performance and how the presented algorithm can capture the uncertainties effects. Note that hereinafter CNT, equivalent fiber and reinforcing agent are used interchangeably for sake of simplicity. Admittedly, readers should distinguish the difference between them during interpretation of the results. For example 7.5% fiber equivalent volume fraction as an output of the optimization algorithm, should be regarded as 5% CNT volume fraction in practice, subtracting the spatial volume of the CNT-polymer interphase region.

6.1 Three-point bending of a beam

The first example is a three point bending beam as shown in Fig. 11 (a). The cross sectional area of the beam is constant along its length. Fig. 11 (b) also depicts the FE mesh while Table-1 indicates all design parameters of the beam. The design constraint is the mid deflection of the beam which should be smaller than an admissible value as mentioned in Table-1.

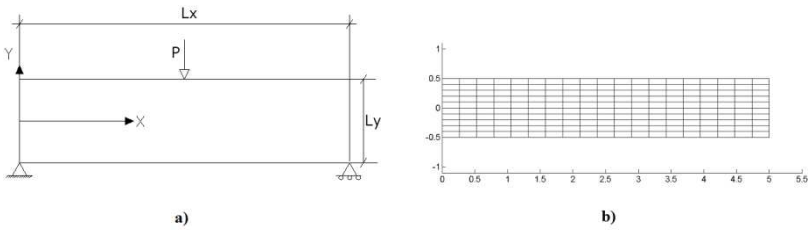

Fig.11. Geometry (a) and FE mesh (b) of a three-point bending beam

Table-1. Problem definitions for the beam under static loading

Parameter	L_x	L_y	E_m	ν_m	P	LSF	β	$Obj.Func.$
Value	5	1	10	0.3	$\mu = 760$ $\sigma = 10$	Max. Deflection $2.5e^{-3}$	3	CNT(volfrac)
Type	D	D	D	D	N	D	D	D

$Length: m,\ E: GPa\ ,\ P: Applied\ load\ (KN),\ \nu: Poisson\ ratio,\ m: matrix\ , volfrac: volume\ fraction$
$D: deterministic, N: normal\ distribution, \mu: mean\ value, \sigma: standard\ deviation\ \ \beta: Reliability\ Index$

Fig. 12 (a) illustrates the reinforcing agent content as optimization objective function versus iterations; while the history of the reliability index is also presented. Fig. 12 (b) shows the same graphs, where the iteration is started from a different point. The, final results are

independent on the iteration start point yielding on optimum at 2.37% reinforcement. Results are based on the assumption of random waviness of the CNT in the resin according to the procedure discussed in Section 2.

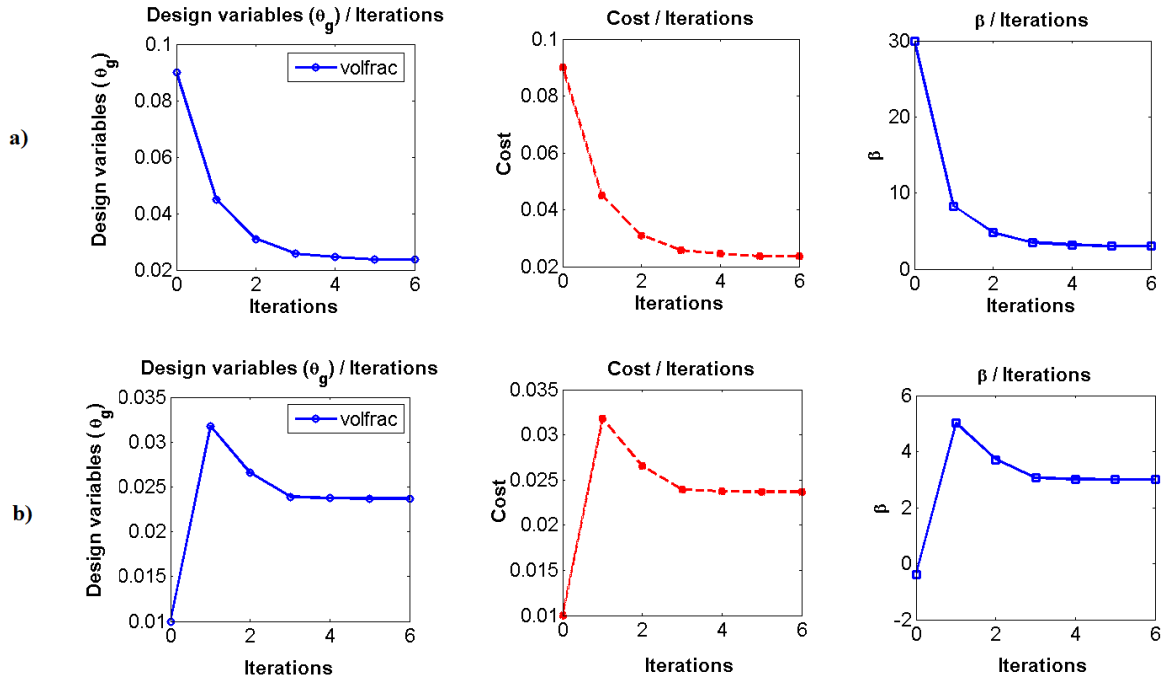

Fig.12. RBDO results of a three-point bending beam with initial guess of reinforcement content 9% (a) and 1% (b), optimum value is 2.37% for both (a) and (b)

Apart from finding the optimum content of the reinforcement agent, it is also important to determine how the uncertainties in the design parameters will affect the reliability of the nanocomposite structures. For this purpose, the CNT waviness and the agglomeration (material design parameters), the applied load (structural parameter) and the FE discretization (modeling parameter), have been selected for more detailed studies. According to [4,5], the waviness is one of the key parameters governing the nanocomposite stiffness. The most influential parameter, the CNT content, has been optimized already.

To analyze the sensitivity of the failure probability with respect to the CNT waviness, other CNT parameters (i.e. length, dispersion, agglomeration and orientation) are considered as random parameters while the resin Young's modulus and its Poisson's ratio are considered as deterministic values because their effects on the overall characteristics of the composite are negligible [4]. Five different levels of waviness have been defined as "waviness intensity" by limiting the upper and lower bounds of longitudinal and transverse stiffness of the RVE. In

the first level (W-1: Very fine waviness), the effective Young's modulus of the CNTRP is a random number between the Young's modulus of the RVEs with the longitudinal and 18 degree aligned CNTs (with respect to longitudinal direction). So, the effective Young's modulus for W-1 has a value between 80% to 100% of the stiffness of the RVE with longitudinally aligned CNTs. Similarly, this concept can be extended to have wavier CNTs (i.e. W-2: fine waviness, W-3: moderate waviness, W-4: severe waviness and W-5: very severe waviness) by setting a limit on the CNT incline angle. Thus W-2, W-3, W-4 imply that the effective Young's modulus of CNTRP has a value between 60% to 100%, 40% to 100% and 20% to 100% of the stiffness of the RVE with longitudinal CNTs, respectively. W-5 also stands for the generic case which effective stiffness of the nanocomposite can take a random value between longitudinal and transverse stiffness of the RVE. Fig. 13 schematically demonstrates the definition of the so called "waviness intensity" concept.

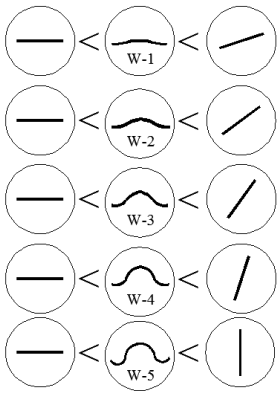

Fig.13. Definition of waviness intensity, a phenomenological concept

Fig. 14 (a) depicts the Young's modulus of the CNTRP versus the reinforcing contents for different waviness intensities. Expectedly, an increase in content of reinforcement or decrease in the CNT waviness yields to higher composite Young's modulus. Fig. 14 (b) shows the reliability index of the beam versus waviness intensity, for the optimum content of the reinforcement (i.e. 2.37%) while other parameters do not experience any variation. Evidently, when the waviness increases, the structural stiffness will decrease. Hence, the beam deflection will increase and consequently the structural reliability will decrease. One should note that for the case of fully wavy CNT (i.e. W-5), the structural reliability is half the reliability of a very fine wavy CNT (i.e. W-1).

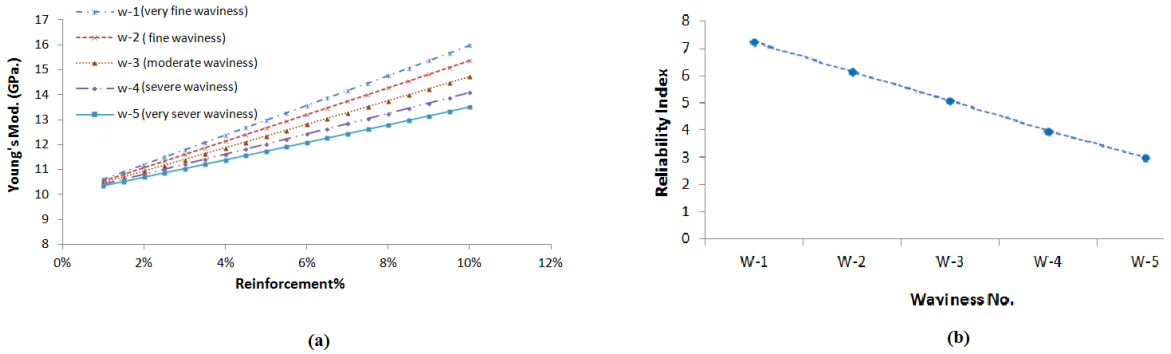

Fig.14. Stiffness of CNTRP versus reinforcement content for different waviness intensities (a) Reliability index of the beam versus waviness (b)

Fig. 15 illustrates the effect of the CNT agglomeration on the reliability of the nanocomposite component. The Young's modulus of CNTRP versus the reinforcement contents for both aggregated and non-aggregated CNTs is plotted in Fig. 15 (a). The CNT agglomeration, reduces the CNTRP stiffness. This reduction is more pronounced for higher values of CNT contents; for CNT contents around 2% and less, the agglomeration role can be neglected. Fig. 15 (b) shows both the failure probability and the reliability index of the beam versus the reinforcement content with and without the CNT agglomeration. Agglomeration also reduces the structural reliability index and increases the failure probability of the structure but as it can be seen from Fig. 15, its effect can be neglected (maximum difference in failure probability considering and disregarding CNT agglomeration is 0.144) without any structural safety concern.

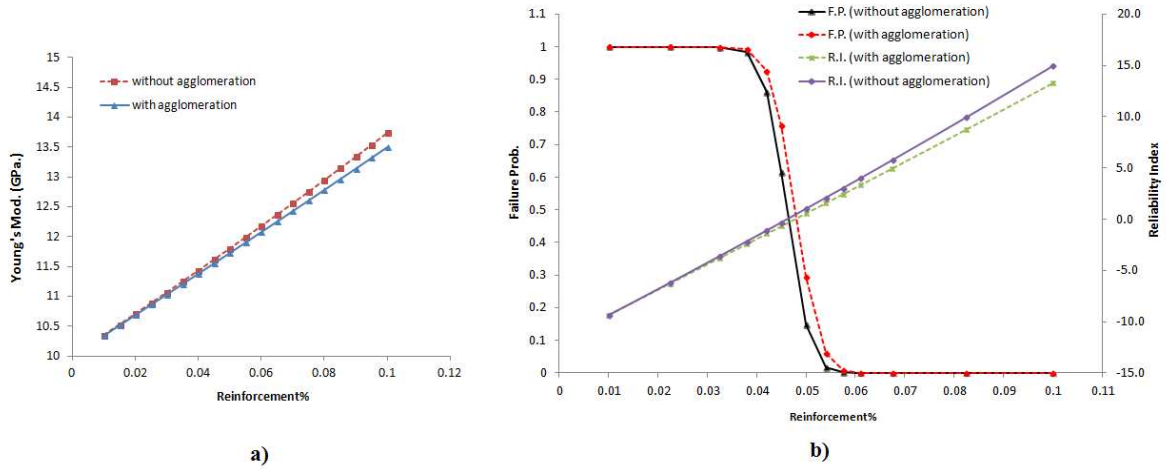

Fig.15. Stiffness of CNTRP versus reinforcement contents with and without CNT agglomeration (a) Reliability index and failure probability of the beam versus reinforcement contents with and without CNT agglomeration (b)

The second category of uncertainties (structural uncertainties) is considered in next step, assuming a fully wavy CNT (i.e. W5). Fig. 16 shows the reliability index and the failure probability of the beam in dependence on the standard deviation of the loading distribution. When the standard deviation increases, the failure probability also increases and β decreases. The rate of the reliability index changes rapidly for small standard deviations and gradually approaches zero (i.e. the system response is not sensitive anymore). An increase in the standard deviation of the loading leads to a more uncertain system that is more susceptible for failure.

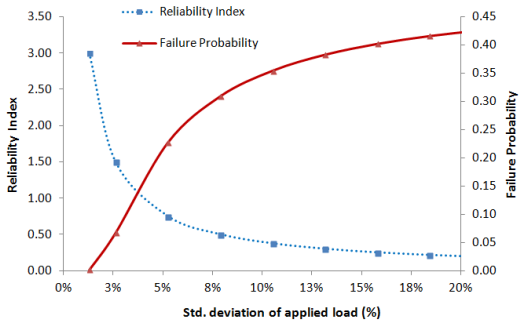

Fig.16. Reliability index and failure probability of the beam versus standard deviation of load

Finally the influence of the discretization on the structural reliability is observed. Fig. 17 depicts the failure probability versus the mesh size parameter, h, which has been defined as the ratio between the beam height and the number of elements in the vertical direction. It could be observed that coarse meshes considerably underestimate the structural failure probability while next to $h = 0.05$, the failure probability reaches a constant value.

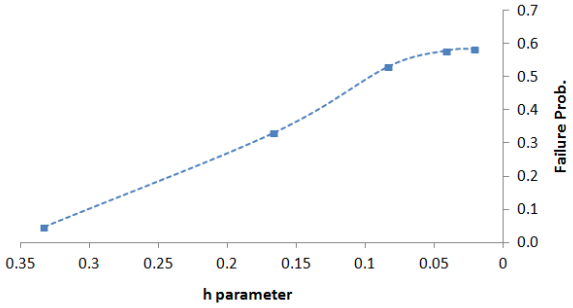

Fig.17. Reliability index versus FE mesh, h, parameter which is defined as the ratio between the beam height and the number of elements in the vertical direction

6.2 Thick cylinder under radial line load

The second example is a thick cylinder under radial distributed loading. Due to geometrical symmetry, only half of the ring is discretized. Fig. 18 (a), (b), (c) and (d) depicts the geometry, loading / boundary conditions, FE discretization and deformed configuration, respectively. Table-2 lists all design parameters. In this example not only the material but also the geometry is simultaneously optimized. At the first step, the minimization of the CNT content and the cylinder thickness as optimization objective function, $1\% < volfrac\% < 10\%$ and $0.1 < t_c < 0.4$ as deterministic design constraints and the maximum transverse deflection with a specified target reliability index (according to Table-2) as stochastic constraint have been taken into account.

Table-2. Problem definitions for thick cylinder under line load

Parameter	R_c	L_c	E_m	ν_m	P	LSF	β	$Obj.Func.$
Value	1	1.5	10	0.3	$\mu = 1000$ $\sigma = 200$	Max. trans. deflect. $7\ e^{-3}$	3	% CNT + t_c
Type	D	D	D	D	N	D	D	D

$Length: m,\ \ E: GPa\ ,\ \ P: Applied\ load\ (KN/m),\ \ \nu: Poisson\ ratio,\ \ m: matrix,\ \ \ \ c: cylinder$

$D: deterministic, N: normal\ distribution, \mu: mean\ value, \sigma: standard\ deviation\ \ \beta: Reliability\ Index$

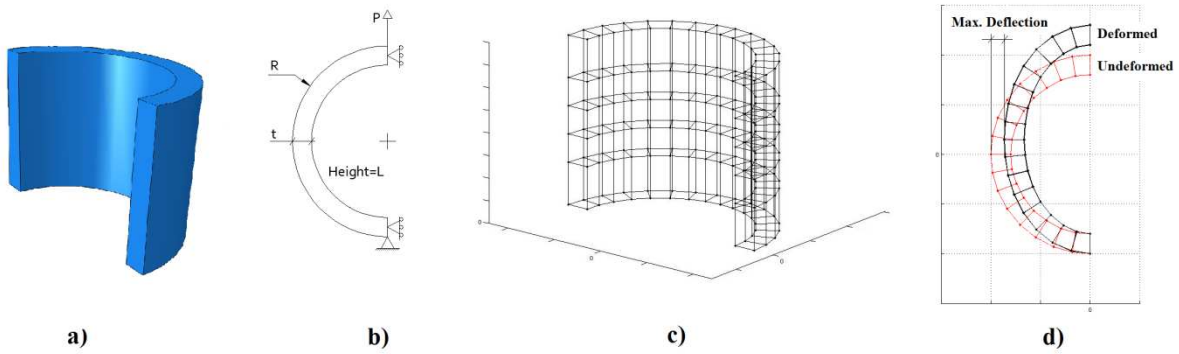

Fig.18. Geometry (a) loading / boundary conditions (b) FE mesh (c) and deformed configuration (d) of a thick cylinder under radial line load

The RBDO results are illustrated in Fig. 19 (a). The optimal thickness and reinforcement content are 0.278 and 1%, respectively. In order to check the correctness of our approach the ring thickness is restricted to an optimum 0.278 in the next simulation. This new constraint is

imposed by changing the deterministic constraints to $1\% < volfrac\% < 15\%$ and $0.1 < t_c < 0.26$. To obtain the same reliability index, the effect of the thickness reduction should be compensated by another design variable, i.e. the CNT content. Fig. 19 (b) shows the results under the new constraints. The optimal thickness now is 0.259 (quite close to constraint's upper limit) while the optimum reinforcement content is increased up to 9.35%.

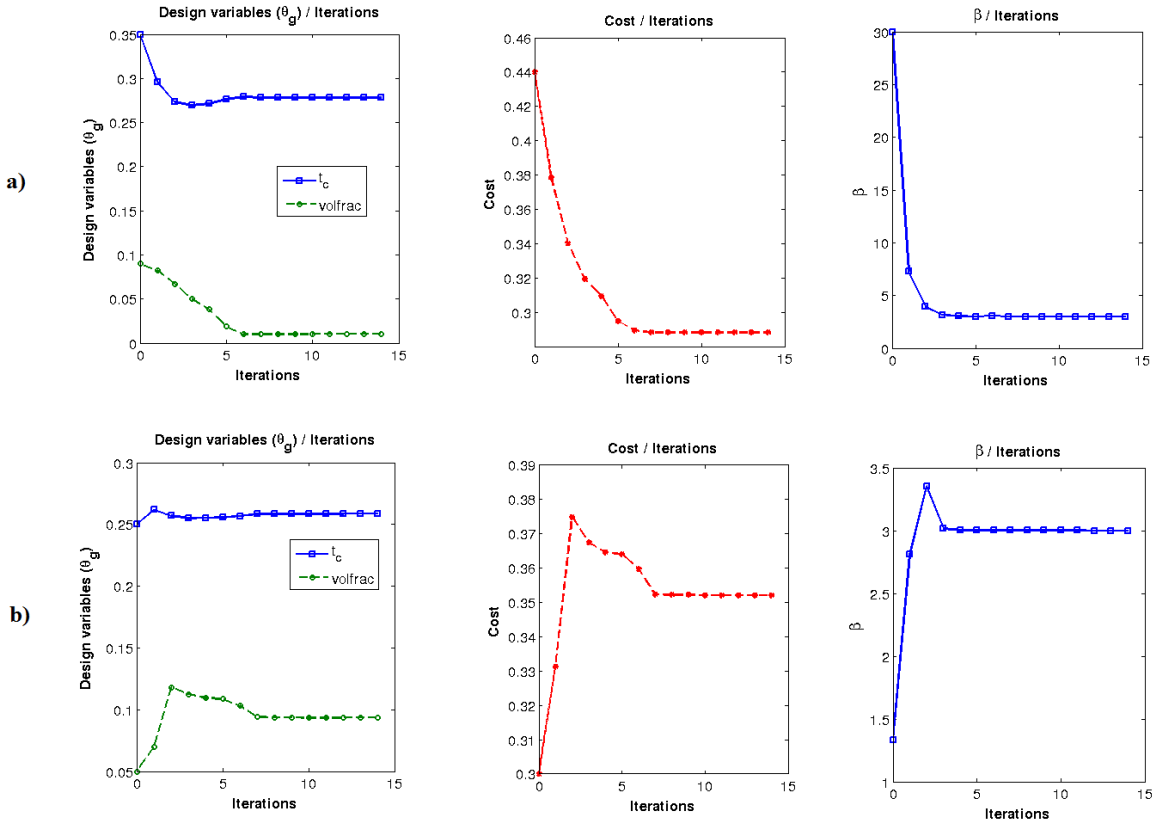

Fig.19. RBDO results of a thick cylinder under radial line load for design constraints as $1\% <$ volfrac$\% < 10\%$ & $0.1 < t_c < 0.4$ (a) $1\% <$ volfrac$\% < 15\%$ & $0.1 < t_c < 0.26$ (b) for both cases t_c and $volfrac$ stand for ring thickness and reinforcement content, respectively

Subsequently, the minimization of both CNT content and cylinder volume have been followed with consideration of the deterministic design constraints $1\% < volfrac\% < 10\%$, $0.1 < t_c < 0.3$, $1.2 < L_c < 1.7$, $0.9 < R_c < 1.1$ and the stochastic design constraint according to Table-2. As Fig. 20 shows, volfrac $= 9.34\%$, $R_c = 0.9333$, $L_c = 1.333$ and $t_c = 0.2032$ are optimal values of the design parameters.

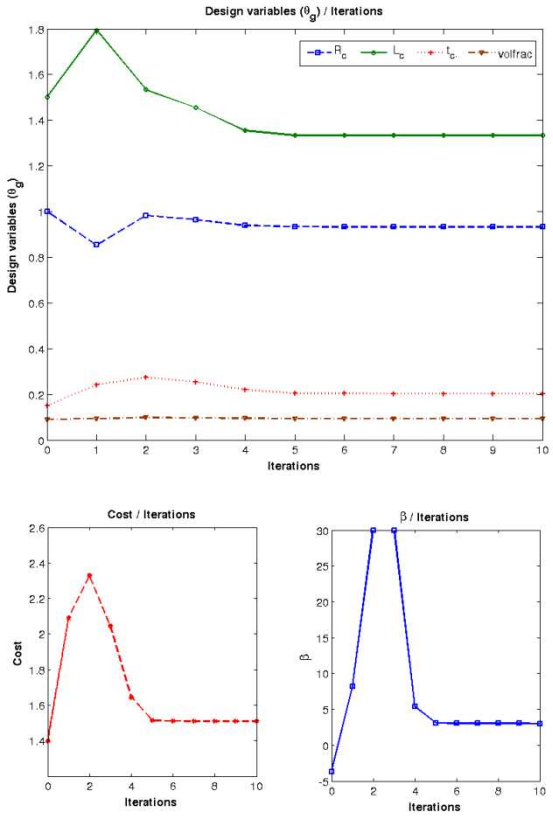

Fig.20. RBDO results of a thick cylinder to find minimum reinforcement content and minimum volume of cylinder including deterministic design constraints as $1\% < \text{volfrac}\% < 10\%$ & $0.1 < t_c < 0.3$ & $1.2 < L_c < 1.7$ & $0.9 < R_c < 1.1$ and stochastic constraint as maximum transverse displacement equal to 0.007 with $\beta = 3$

7. Conclusions

Deterministic approaches for nanocomposite modeling and optimization might be unrealistic for certain applications and may yield to either catastrophic failure or unnecessary conservatism. Although probabilistic approaches can cover uncertainties effects, their implementations do not necessarily yield reliable nanocomposite designs. Detailed investigations on uncertainties and their propagation should be performed for realistic and reliable PNC structures. Uncertainty propagation over different length scales and through various sources have been addressed for nanocomposite components. Potential uncertainties have been categorized in material, structural and modeling levels. To fully address uncertainties in material level, a stochastic multi-scale material model (which includes all important aspects of the CNTRP including CNT length, orientation, dispersion, agglomeration and waviness, at different length scales from nano- up to macro-scale) has been utilized. To improve the computational efficiency, the evaluation of material properties

has been surrogated by a metamodel. The results for two selected examples show that the failure probability of a polymeric nanocomposite structure, strongly depends on the CNT parameters, especially the CNT volume fraction and the waviness. The influence of the CNT agglomeration is nearly negligible. It was observed that neglecting the CNT agglomeration can simplify the model and decrease the computational time without remarkable loss in model accuracy. Furthermore, the loading condition and discretization affect the reliability of the system. Coarse meshes underestimate the failure probability of a beam while fine meshes admittedly increase computational cost. Thus sufficiently refined discretization should be investigated in order to have realistic assessment of the reliability of PNC structures. An increase in the standard deviation of the applied load, which physically means more uncertainties in the system, resulted in the structure with a smaller reliability index. Finding the optimal content of CNT was also presented to optimized the material instead of the geometry. As a further step forward, concurrent optimization of material parameters and geometrical parameters (hybrid optimization) was conducted to present a comprehensive solution for current demands in fully optimized designs of nanocomposite components.

Acknowledgments:

This work was supported partially by Marie Curie Actions under the grant IRSES-MULTIFRAC and German federal ministry of education and research under the grant BMBF SUA 10/042. Nachwuchsförderprogramm of Ernst Abbe foundation is also acknowledged.

References:

[1] Lau KT, Gu C, Hui D, A critical review on nanotube and nanotube/nanoclay related polymer composite materials, Compos: Part B–Eng. 37 (2006) 425-436.

[2] M.M. Shokrieh, R. Rafiee, A review of the mechanical properties of isolated carbon nanotubes and carbon nanotube composites, Mechanics of composite materials 46, No.2 (2010) 229-252.

[3] M.M. Shokrieh, R. Rafiee, Development of a full range multi-scale model to obtain elastic properties of CNT/polymer composites, Iranian polymer journal 21 (2012) 397-402.

[4] M. Rouhi, M. Rais-Rohani, Modeling and probabilistic design optimization of a nanofiber-enhanced composite cylinder for buckling, Composite structures 95 (2013) 346-353.

[5] M.M. Shokrieh, R. Rafiee, Stochastic multi-scale modeling of CNT/polymer composites, Computational material science 50 (2) (2010) 437-446.

[6] M.M. Shokrieh, R. Rafiee, Prediction of mechanical properties of an embedded carbon nanotube in polymer matrix based on developing an equivalent long fiber, Mechanics research communications 37 (2010) 235–240.

[7] M.M. Shokrieh, R. Rafiee, Investigation of nanotube length effect on the reinforcement efficiency in carbon nanotube based composites, Composite Structures 92 (2010) 2415–2420.

[8] D.L. Shi, X.Q. Feng, Y.Y. Huang, K.C. Hwang, H. Gao, Eng. Mater – T. ASME 126

(2004) 250–257.

[9] T. Mori, K. Tanaka, Acta Metall. Sin. 21 (1973) 71–575.

[10] M.Chiachio, J.Chiachio, G.Rus, Reliability in composites - A selective review and survey of current development, Composites 43(B) (2012) 902-913.

[11] Hasofer, A.M. and Lind N., An Exact and Invariant First-Order Reliability Format, Journal of Engineering Mechanics ASCE 100 (1974) 111-121.

[12] Hong-Seok Park, Xuan-Phuong Dang, Structural optimization based on CAD-CAE integration and metamodeling techniques, Computer-Aided Design 42 (2010) 889-902.

[13] Santner T.,Williams B., Notz W., The design and analysis of computer experiments, Springer series in Statistics, Springer (2003)

[14] S.N. Lophaven, H.B. Nielsen, J. Sondergaard, DACE a Matlab kriging toolbox version 2.0, Technical Report IMM-TR-2002-12, Informatics and mathematical modeling, DTU (2002)

[15] J.-M. Bourinet, FERUM 4.1 user's guide, (2010) available online at: http://www.ifma.fr/cache/offonce/lang.